High-pressure crystal structure prediction of calcium borohydride using density functional theory

Philippe C. Aeberhard,[1,*] Keith Refson,[2] Peter P. Edwards,[1] and William I. F. David[1,2,†]
[1]*Department of Chemistry, ICL, University of Oxford, South Parks Road, Oxford OX1 3QR, United Kingdom*
[2]*ISIS Facility, Rutherford Appleton Laboratory, Chilton, Oxfordshire, OX11 0QX, United Kingdom*
(Received 28 January 2010; revised manuscript received 11 June 2010; published 6 May 2011)

Three high-pressure polymorphs of the hydrogen storage material calcium borohydride [$Ca(BH_4)_2$] are predicted from structural analogs of the high-pressure titanium dioxide (TiO_2) polymorphs baddeleyite, columbite, and cotunnite. Their phase stabilities with respect to the three experimentally characterized polymorphs α, β, and γ are determined by accurate density functional theory calculations of their thermodynamic equations of state. Although these structures have not yet been observed experimentally, it is found that the proposed $Ca(BH_4)_2$ polymorphs are thermodynamically stable (at 0 K) at pressures above 3.6 GPa and that the ordering of the phase stabilities with respect to pressure is similar to TiO_2.

DOI: 10.1103/PhysRevB.83.174102 PACS number(s): 61.50.Ks, 61.50.Ah

I. INTRODUCTION

The safe and efficient storage of hydrogen is one of the major technical problems to be solved for an alternative hydrogen-based energy economy to become reality. Hydrogen storage in solids is generally regarded as being a most promising way of meeting the conditions for technically applicable storage requirements. The complex metal hydrides form a class of hydrogen storage compounds that could potentially meet the gravimetric and volumetric storage requirements.[1] Calcium borohydride, $Ca(BH_4)_2$, is one such prospective hydrogen storage material, with a total hydrogen content of 11.6% by mass, and an available hydrogen content of 9.6% by mass for decomposition to calcium hydride and calcium hexaboride,

$$3Ca(BH_4)_2(s) \rightarrow CaB_6(s) + 2CaH_2(s) + 10H_2(g). \quad (1)$$

The standard reaction enthalpy of the above decomposition reaction has been calculated *ab initio* as $\Delta H^\circ = 35.2$ kJ/mol, corresponding to a favorable decomposition temperature of about 94 °C under 1 bar hydrogen.[2] In practice, however, calcium borohydride decomposes only at elevated temperatures of 350 °C,[3] indicating a high kinetic barrier to decomposition.

Calcium borohydride is a crystalline solid that forms a number of different polymorphs. Four different polymorphs have been observed, and the crystal structures are known for three of them (Table I), named α (α' at high temperature), β, and γ phases. A remarkable structural similarity exists between the observed polymorphs of $Ca(BH_4)_2$ and the known ambient-pressure polymorphs of TiO_2—rutile, anatase, and brookite. $Ca(BH_4)_2$ is analogous to TiO_2 in the following four respects. First, $Ca(BH_4)_2$ is essentially an ionic crystal composed of Ca^{2+} and BH_4^- ions, and is isoelectronic with titanium dioxide, TiO_2, which consists of Ti^{4+} and O^{2-} ions. Second, the ratios of the ionic radii of cations and anions in both compounds are similar: In TiO_2, the ratio of the Ti^{4+} ionic radius and the average Ti-O bond length is 0.31, and in $Ca(BH_4)_2$ the ratio of the Ca^{2+} ionic radius and the average Ca-B distance in the first coordination shell is 0.34. A difference lies in the cation-anion bond lengths: The Ca-B distance is on average 1.50 times longer than Ti-O, a fact that is reflected in the lattice parameters, which are on average 1.50 times longer in $Ca(BH_4)_2$ than in corresponding TiO_2 polymorphs. Third, Fig. 1 illustrates that the cation-anion binding potentials have very similar shapes around the equilibrium distance, taking into account the different lattice parameters in the bulk materials. For this reason, it can be expected that very similar structures will occur not only at ambient pressure, but also at high pressure. For comparison, Fig. 1 contains the same binding curves for the ion pairs Ca^{2+}-Br^- and Mg^{2+}-BH_4^-. $CaBr_2$ has been previously used as a model for $Ca(BH_4)_2$ phases[10] on the grounds of a similar, rutile-type, polymorph and on the similar ionic radii of Br^- and BH_4^-. However, the ionic binding curves in Fig. 1 do not show the same level of similarity to Ca-BH_4 as Ti-O; likewise, if we replace the cation by Mg^{2+}, a binding curve much different from Ca-BH_4 is obtained. This shows that both the cation and the anion need to share similar properties, and this is the case for TiO_2 more than for the other ion pairs due to the fact that they are isoelectronic. Finally, a closer look shows that the electronic structure of the bonds in both compounds bear similarities: The cations have the electronic configuration [Ar] and are able to accept a certain amount of electron density to the empty *d* orbitals. Figure 2 shows the partial electronic densities of states (eDOS), projected on the cation sites, in rutile-structured $Ca(BH_4)_2$ and TiO_2. *d*-electron character is clearly present in $Ca(BH_4)_2$ and $CaBr_2$. If Ca atoms are replaced by Mg atoms, the *d* character vanishes in the resulting hypothetical structure. Figure 3 shows four isosurface plots of the difference between the sum of electron densities of unperturbed atoms and the actual electron density of the crystal (all electron densities calculated by DFT) around the cations for TiO_2, $Ca(BH_4)_2$, $Mg(BH_4)_2$, and $CaBr_2$, all in the rutile structure. From these electron density difference plots it is seen that *d* character is present for TiO_2 and for compounds with a calcium cation, but none is seen for $Mg(BH_4)_2$. It is important that the cation have accessible electronic *d* levels for this similarity; however, this is in itself not a sufficient criterion as shown by the case of $CaBr_2$, which has *d*-electron character on the calcium sites, but no known polymorphs similar to TiO_2 other than the rutile structure. Łodziana and van Setten have very recently published a more in-depth theoretical study focusing on the metal-BH_4^- interaction in alkali and alkaline-earth borohydrides.[11]

These qualitative parallels between these two compounds have previously led us to a structural comparison, where we found that the crystal structures of rutile, anatase, and

TABLE I. The crystal polymorphs of $Ca(BH_4)_2$ that have been experimentally observed. XPD: laboratory x-ray powder diffraction. SXPD: synchrotron x-ray powder diffraction. NPD: neutron powder diffraction. DFT: *ab initio* structure prediction using density functional theory.

Phase	Space group	Structure determination	Reference
α	$Fddd$, $F2dd$	SXPD, XPD	4 and 5
α'	$I4_1/amd$, $I\bar{4}2d$	SXPD	5
β	$P4_2/m$, $P\bar{4}$	SXPD, NPD	5 and 6
γ	$Pbca$	SXPD, NPD, DFT	6–8
δ		(not solved)	9

brookite TiO_2 polymorphs are remarkably similar to the known α/α', β, and γ polymorphs of $Ca(BH_4)_2$, respectively.[7] *Ab initio* crystal structure predictions of $Ca(BH_4)_2$ have been carried out before using different approaches. Vajeeston *et al.*[12] constructed $Ca(BH_4)_2$ analogs from a large number of database crystal structures of chemical formula MX_2Y_8 (with M being any metal) with CaB_2H_8 chemistry, and subsequently optimized the geometries of these analogs by DFT. They identified multiple plausible crystal structures, including the experimental ground state (the α phase), but none of the other experimental structures that have since been determined. Majzoub and Rönnebro[13] used their prototype electrostatic ground state (PEGS) method to efficiently generate physically sensible starting structures using a simple electrostatic Hamiltonian and the Metropolis Monte Carlo method; the geometries of these prototype structures were then optimized by DFT. Using this method, the authors were able to predict the experimentally known structures, but they did not correctly predict the structure of the γ phase, which was only later determined experimentally.[8] Nakamori *et al.*[10] predicted borohydride structures using a similar comparative argument, likening the structures borohydrides of Ca, Mg, and Zn to those of the corresponding bromides and iodides with the same metal cation, arguing that the ionic radius of BH_4^- is closest to Br^- and I^-; however, these halides do not show the same polymorphism as the halides, showing that the ionic radius alone is not enough to give rise to the same crystal structures. None of the above-mentioned computational studies attempt to address high-pressure $Ca(BH_4)_2$ crystal structures and properties directly.

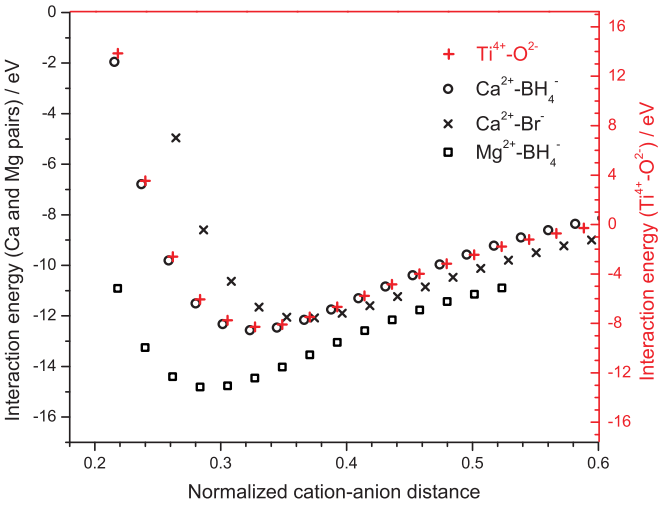

FIG. 1. (Color online) Calculated interaction energy between isolated gas phase cation-anion pairs [Becke three-parameter Lee-Yang-Parr (B3LYP)/6-311+G(d) using Gaussian03]. The cation-anion distance was divided by the lattice parameter a of the rutile crystal structure of the corresponding bulk compound; the energy axis for Ti-O was scaled for better comparison. The position of the binding energy minimum and the short-range behavior of the energy curves are similar for Ti-O and Ca-BH_4. Ti-O is more similar to Ca-BH_4 than is Ca-Br or Mg-BH_4, therefore we expect $Ca(BH_4)_2$ polymorphism to be similar to that of TiO_2.

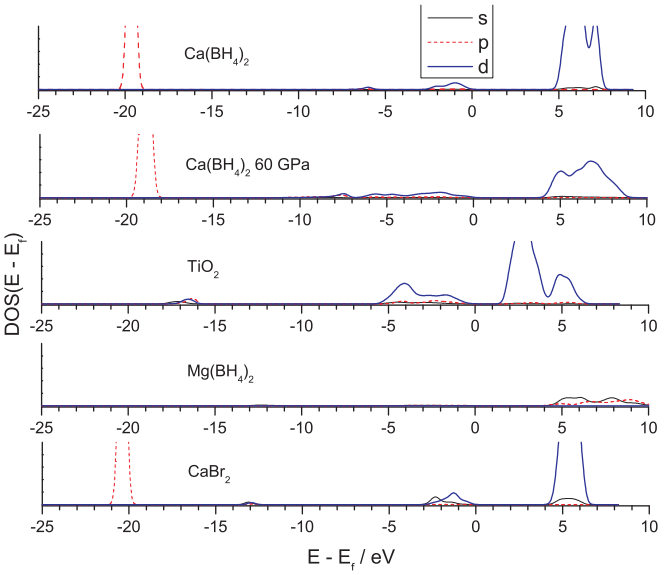

FIG. 2. (Color online) The electron density of states for $Ca(BH_4)_2$, TiO_2, CaBr, and $Mg(BH_4)_2$, all in the rutile structure, shown as angular momentum-decomposed density of states plots projected on the metal cation. The valence bands all show significant d character except when the cation is not Ca^{2+} or Ti^{4+}.

In this paper, the high-pressure phase stabilities of calcium borohydride are investigated by *ab initio* structural modeling using state-of-the-art density functional theory (DFT) calculations. We complete the TiO_2-$Ca(BH_4)_2$ structural analogy and predict three possible polymorphs of $Ca(BH_2)_2$ based on the three high-pressure polymorphs of TiO_2 as templates; these are baddeleyite, columbite, and cotunnite. Calculations focus on the equations of state in the low-temperature limit (0 K), but include the nuclear zero-point vibrational contributions to the free energy.

Two experimental studies of $Ca(BH_4)_2$ under high pressure have so far been published,[14,15] which investigated the structural behavior of the α and β phases under pressures up to 25 GPa and room temperature by x-ray powder diffraction and Raman spectroscopy; no transitions into different crystalline polymorphs were observed for either phase, but the β phase was observed to transform into an unknown disordered or amorphous phase.

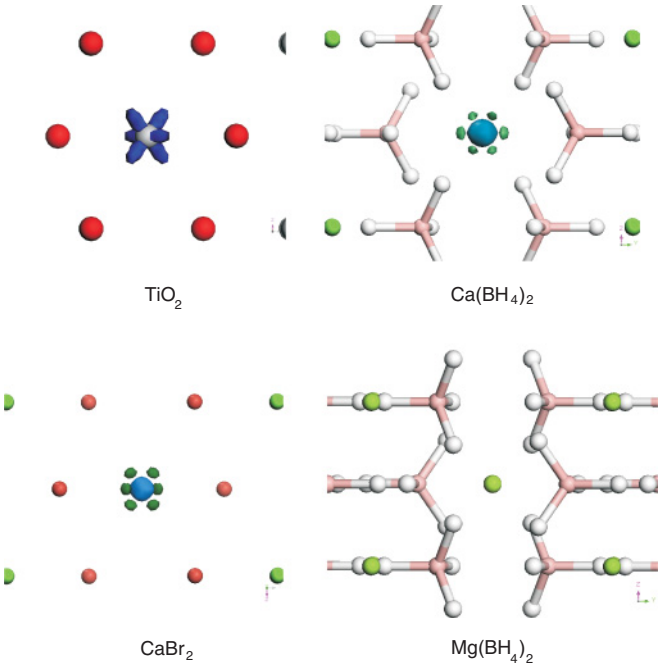

FIG. 3. (Color online) Isosurface plots of the calculated electron density difference (sum of the electron densities of the free atoms, subtracted from the total electron density of the crystal) for rutile-type structures of various chemistries; all atom positions and cell parameters were optimized by DFT. The similar d-electron character on the metal cation is clearly visible in TiO_2 and the calcium compounds, but it is completely absent in $Mg(BH_4)_2$.

II. COMPUTATIONAL METHODS

All structural calculations were carried out using DFT in the Kohn-Sham formalism[16] as implemented in the CASTEP[17] simulation package. The Kohn-Sham orbitals of the valence electrons are expressed in a plane-wave basis set, and atomic pseudopotentials are used to represent the core electrons of each atom. The Perdew-Burke-Ernzerhof functional for exchange and correlation[18] was employed in all calculations.

Structural optimizations were performed by minimizing the forces on each atom until they were all lower than 0.01 eV/Å. The cell stress was simultaneously optimized until it differed from the target cell stress by less than 0.05 GPa. Ultrasoft pseudopotentials were used for these structural calculations with a plane-wave kinetic energy cutoff of 340 eV and a Fourier grid with a maximum reciprocal range of 20 $Å^{-1}$. The Brillouin zone for electronic integration was sampled on a regular Monkhorst-Pack grid[19] with a maximum spacing of 0.04 $Å^{-1}$ between sampling points for every structure; the grid sizes effectively used were: $5 \times 4 \times 7$ for the α phase, $4 \times 4 \times 6$ for the β phase, $2 \times 4 \times 4$ for the γ phase, $4 \times 4 \times 4$ for columbite and baddeleyite, and $4 \times 6 \times 3$ for cotunnite. The pseudopotentials were generated according to the Vanderbilt ultrasoft scheme[20] with a valence atomic number of 1 for hydrogen, 3 for boron, and 10 for calcium. The cutoff radii for the pseudopotentials were chosen so that the core regions of neighboring atoms (especially B and H) do not overlap.

The zero-point energy (ZPE) from nuclear vibrations was taken into account and was calculated from the phonon density of states (PDOS) of each structure.[21] The phonon frequencies were calculated using the density functional perturbation theory method (DFPT),[22] also implemented in CASTEP. Phonon frequencies were calculated on a coarse grid of **q** vectors in the Brillouin zone and subsequently interpolated on a finely spaced grid of **q** vectors using Fourier interpolation to obtain an accurate PDOS. We have found that phonon dispersion is very low in all $Ca(BH_4)_2$ structures, and this interpolation scheme is both highly efficient and precise. All phonon frequency calculations were performed using norm-conserving pseudopotentials with a plane-wave cutoff energy of 850 eV. Norm-conserving pseudopotentials were generated according to the optimized pseudopotential scheme[23] using the same core configuration as in the ultrasoft case.

The plane-wave cutoff of 340 eV with ultrasoft pseudopotentials (850 eV for norm-conserving pseudopotentials) was chosen so that the residual convergence error was less than 0.1 eV in the energy, 0.01 eV/Å in the force, and 0.1 GPa in the stress. Similarly, the Brillouin-zone sampling was chosen to achieve a convergence of better than 1 meV in energy, 0.005 eV/Å in the force, and 0.1 GPa in stress.

III. RESULTS AND DISCUSSION

A. Baddeleyite, columbite and cotunnite $Ca(BH_4)_2$ structures

We attempt to predict three possible polymorphs of $Ca(BH_4)_2$ by finding the equilibrium geometries by DFT geometry optimization and testing for the presence of imaginary phonon frequencies which would indicate a mechanically unstable structure.

$Ca(BH_4)_2$ structural analogs of the three high-pressure polymorphs of TiO_2 were constructed, placing the Ca atoms at Ti sites and B atoms at O sites, and retaining the full space group symmetry ($P2_1/c$ for baddeleyite,[24] *Pbcn* for columbite,[25] and *Pnma* for cotunnite[26]). The unit-cell parameters were scaled such that the initial Ca-B distance had the value of the average from the known α-γ polymorphs, ~2.9 Å. Hydrogen atoms were arranged in regular tetrahedra around B atoms with an initial B-H bond length of 1.20 Å. For cotunnite $Ca(BH_4)_2$, the BH_4 units are centered on Wyckoff positions 4c with site symmetry m, implying that there are two possible orientations of the tetrahedral hydrogen positions. In baddeleyite and columbite, the BH_4 units are located on general positions with no site symmetry and thus an infinite number of orientations is possible. In these cases ten different starting structures with randomly oriented BH_4 units were generated and their geometries optimized. The structure with the lowest enthalpy was then selected as the ground-state structure. The geometries were optimized by minimizing the forces on all atoms and the cell stress difference from the external pressure as described in the previous section. Initially, an external pressure of 60 GPa was set for the three high-pressure structures, and 0 GPa for the three ambient pressure structures.

To obtain the energy as a function of volume, each structure (unit-cell parameters and atom positions) was then reoptimized at 12 different external pressures; these ranged between 0 and 30 GPa for α, 0 and 60 GPa for β and γ, 20 and 60 GPa for baddeleyite and columbite, and 40 and 60 GPa

TABLE II. Calculated unit-cell parameters and fractional atomic positions for baddeleyite, columbite, and cotunnite $Ca(BH_4)_2$ at their highest stable volume (see Sec. III B).

Baddeleyite $Ca(BH_4)_2$, space group $P2_1/c$ (No. 14) $a = 7.0201$ Å, $b = 6.3637$ Å, $c = 7.9061$ Å, $\beta = 91.6407^\circ$			
Atom (Wyckoff pos.)	x	y	z
Ca (4*e*)	0.73680	0.51920	0.36710
B (4*e*)	0.57860	0.24040	0.59090
B (4*e*)	0.07290	0.19840	0.83530
H (4*e*)	0.40130	0.92160	0.85830
H (4*e*)	0.46440	0.73590	0.05950
H (4*e*)	0.26890	0.65270	0.89030
H (4*e*)	0.54910	0.65490	0.83380
H (4*e*)	0.07510	0.78070	0.62340
H (4*e*)	0.79630	0.79890	0.59890
H (4*e*)	0.91640	0.51490	0.62120
H (4*e*)	0.91830	0.69010	0.81820
Columbite $Ca(BH_4)_2$, space group *Pbcn* (No. 60) $a = 6.1909$ Å, $b = 7.1905$ Å, $c = 6.4862$ Å			
Atom (Wyckoff pos.)	x	y	z
Ca (4*c*)	1/2	0.34060	3/4
B (8*d*)	0.73990	0.09110	0.54960
H (8*d*)	0.66090	0.81250	0.91710
H (8*d*)	0.38270	0.32410	0.36240
H (8*d*)	0.10400	0.46120	0.33310
H (8*d*)	0.19010	0.95440	0.03440
Cotunnite $Ca(BH_4)_2$, space group *Pnma* (No. 62) $a = 6.9124$ Å, $b = 3.6695$ Å, $c = 7.8723$ Å			
Atom (Wyckoff pos.)	x	y	z
Ca (4*c*)	0.27890	1/4	0.15450
B (4*c*)	0.50270	1/4	0.83560
B 4c)	0.13070	3/4	0.96510
H (4*c*)	0.90470	1/4	0.88990
H (4*c*)	0.43810	3/4	0.02400
H (4*c*)	0.99830	3/4	0.87620
H (4*c*)	0.86440	3/4	0.24130
H (8*d*)	0.21520	0.01310	0.92330
H (8*d*)	0.92030	0.52300	0.68190

for cotunnite. No convergence was obtained for pressures above 30 GPa for the α phase or for pressures below the lower limit indicated for the high-pressure phases. The total energies at various volumes can then be used to determine

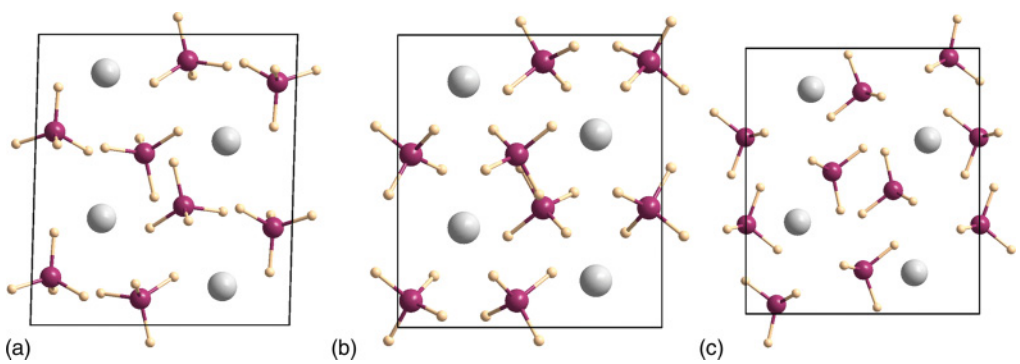

FIG. 4. (Color online) The equilibrium geometries for (a) baddeleyite, (b) columbite, and (c) cotunnite $Ca(BH_4)_2$ calculated by DFT.

the thermodynamical equilibrium volume (see Sec. III B). The resulting cell parameters and atomic positions for the three high-pressure phases are presented in Table II and the structures are shown in Fig. 4.

There were no significant differences between the structures before and after optimization and all phonon frequencies were real and positive, indicating mechanically stable structures. The optimized structures had ground-state energies comparable to the experimentally known polymorphs, making these three structures plausible high-pressure crystal polymorphs of $Ca(BH_4)_2$.

B. Thermodynamic stability with pressure

In order to obtain the thermodynamic stabilities of each structure at 0 K, the total internal energy was calculated as a function of volume. The total internal energy for a crystalline phase consists of the quantum mechanical electronic energy and the energy of the nuclear vibrations (phonons) at zero temperature (the ZPE). The total energy was calculated at ten different volumes for each phase. Calculations of the ZPE are computationally very demanding and were done for only three to four different volumes per structure. Because the ZPE varies smoothly with volume, it was interpolated by a quadratic function to obtain the ZPE at all volumes. The total energy was thus calculated as

$$E(V) = E_{\mathrm{DFT}}(V) + \mathrm{ZPE}(V). \tag{2}$$

$E_{\mathrm{DFT}}(V)$ is the total (static) electronic energy calculated from DFT, and $\mathrm{ZPE}(V)$ is the interpolated ZPE at volume V.

The calculated total energy $E(V)$ with ZPE correction as a function of volume for each structure was fitted to the third-order Birch-Murnaghan equation of state for solids[27,28] [Eq. (3)], providing the bulk modulus and equilibrium volume for each structure. Excellent fits were obtained in each case:

$$E(V) = E_0 + \frac{9B_0V_0}{16}\left\{B_0'\left[\left(\frac{V_0}{V}\right)^{2/3} - 1\right]^3 + \left[\left(\frac{V_0}{V}\right)^{2/3} - 1\right]^2\left[6 - 4\left(\frac{V_0}{V}\right)^{2/3}\right]\right\}. \tag{3}$$

E_0 and V_0 are, respectively, the energy and the volume at equilibrium (zero pressure), B_0 is the bulk modulus at equilibrium, and B_0' is the pressure derivative of the bulk modulus at equilibrium.

Figure 5 shows the fitted equations of state, Eq. (3), for all six phases. Table III lists the equation-of-state parameters for all phases from the fit. The unit-cell parameters for

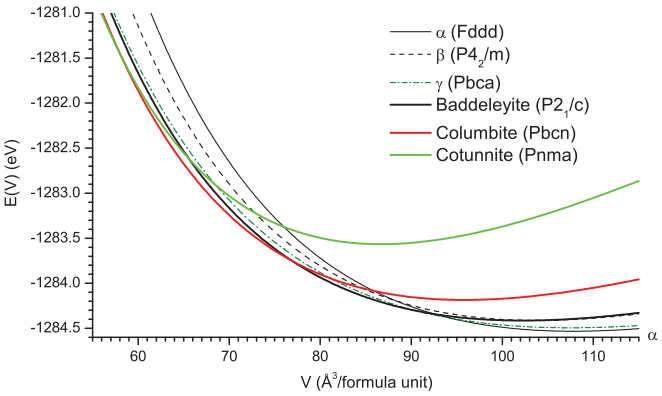

FIG. 5. (Color online) The equation of state (fitted to the calculated total energy with ZPE correction) for all six phases of $Ca(BH_4)_2$ as a function of volume.

the α, β, and γ agree with experimental values to within 0.2%–0.9%.

The α phase is the only polymorph for which the bulk modulus has been measured experimentally. The value found by George *et al.*[14] is $B_0 = 22.95(4)$GPa [and $B_0' = 2.63(0.5)$] and compares well with our results; the discrepancy in the pressure derivative of the bulk modulus is caused by small systematic errors in the calculated energy at different volumes that have a large effect on B_0'.

We found that the ZPE is an essential contribution to the internal energy in order to establish an accurate energy-volume curve. Omitting the ZPE altogether leads to a large error in the estimated equilibrium volume and to a wrong energy offset E_0, to which the determination of phase transition pressures between phases is very sensitive. The ZPE also varies significantly, though slowly, with volume, and therefore it is not sufficient to take the ZPE into account in the form of a simple constant energy offset per phase.

The phase stability with respect to pressure, at a temperature of 0 K, is summarized in Table IV. Transition pressures between two phases are calculated from the energy versus volume plot of Fig. 5 by calculating the negative slope of common tangents to the two corresponding curves. Phase transition pressures deduced by this method are very sensitive to errors in the absolute energies of the two curves and should therefore be considered as approximate values only.

Our calculations indicate that the experimentally well-known β phase is thermodynamically unstable with respect to other polymorphs at any pressure in the low-temperature

TABLE III. Calculated cell parameters of $Ca(BH_4)_2$ phases from Birch-Murnaghan equation of state fitting. B_0 is the bulk modulus at zero pressure, B_0' is the pressure derivative of B_0, and V_0 and E_0 are, respectively, the volume and relative energy per formula unit at zero pressure.

Phase	Cell parameters at zero pressure	B_0 (GPa)	B_0'	V_0 (Å^3/f.u.)	E_0 (eV/f.u.)
α (*Fddd*)	$a = 8.7643$ Å, $b = 13.1485$ Å, $c = 7.4852$ Å	21.8	4.1	107.82	0 (by def.)
γ (*Pbca*)	$a = 13.2425$ Å, $b = 8.5639$ Å, $c = 7.5799$ Å	17.3	4.0	107.45	+0.0379
Baddeleyite ($P2_1/c$)	$a = 7.3720$ Å, $b = 6.6760$ Å, $c = 8.3107$ Å, $\beta = 89.2294$	21.2	4.0	102.24	+0.1186
β ($P4_2/m$)	$a = 6.8842$ Å, $c = 4.3827$ Å	22.9	4.0	103.85	+0.1204
Columbite (*Pbcn*)	$a = 6.8750$ Å, $b = 7.9194$ Å, $c = 7.0403$ Å	25.9	4.0	95.83	+0.3474
Cotunnite (*Pnma*)	$a = 8.3355$ Å, $b = 4.2825$ Å, $c = 9.7102$ Å	38.3	3.8	86.66	+0.9666

TABLE IV. Phase transition pressures at 0 K. Note that the β phase, $P4_2/m$, is not stable at this temperature.

Most stable phase	Pressure range of stability (GPa)
α (*Fddd*)	<3.4
γ (*Pbca*)	3.4–3.6
Baddeleyite ($P2_1/c$)	3.6–9.7
Columbite (*Pbcn*)	9.7–34.0
Pnma	>34.0

limit. This agrees with the observation by Fichtner *et al.* that the β phase is metastable at room temperature[29] and slowly transforms into the α phase. This is also in agreement with the high-pressure results by George *et al.*,[14] who find that the β phase irreversibly transforms into an unknown disordered or amorphous phase as pressure is applied and does not seem to transform back into any crystalline phase at ambient pressure.

IV. CONCLUSIONS

We have predicted three high-pressure polymorphs of calcium borohydride based on an observed structural analogy with titanium dioxide polymorphs and calculated their ground-state structures using density functional theory methods. The three polymorphs correspond to the baddeleyite, columbite, and cotunnite structures and are predicted to be stable at pressures of approximately 3.6 GPa and higher.

We have added a theoretical justification and basis to the structural similarity between TiO_2 and $Ca(BH_4)_2$ by showing that the binding energies at short distances between Ca^{2+} and BH_4^- are related to those between Ti^{4+} and O^{2-} by a simple scaling law; the structural similarity of $Ca(BH_4)_2$ to TiO_2 can therefore also be observed for high-pressure structures. Baddeleyite and columbite structures form at elevated pressures for both phases: in TiO_2, the columbite phase forms at 2.5 GPa, and the baddeleyite phase at 12 GPa,[24] whereas in $Ca(BH_4)_2$ baddeleyite is predicted to be the most stable phase at pressures above 3.6 GPa and columbite above 9.7 GPa. Both $Ca(BH_4)_2$ and TiO_2 form cotunnite phases at much higher pressures [60 GPa for TiO_2,[26] and 34 GPa for $Ca(BH_4)_2$].

We have calculated the thermodynamic energy-volume relationship to establish the phase stabilities of the predicted polymorphs, as well as of three experimentally well-known polymorphs that are stable (or metastable) at low temperature. Calculated unit-cell parameters and bulk moduli correspond well to reported experimental values where known, with the exception of the pressure derivative of the bulk modulus (B_0'), which is measured and calculated with a large uncertainty that does not affect the quality of the fit strongly.

It was found that the zero-point vibrational contributions to the total energy are essential in order to estimate equilibrium volume parameters accurately.

ACKNOWLEDGMENTS

Computing resources were provided by the Science and Technology Facilities Council's (STFC) e-Science facility and by the Oxford Supercomputing Center. P. C. A. acknowledges the Engineering and Physical Sciences Research Council and STFC for financial support.

*philippe.aeberhard@chem.ox.ac.uk
†bill.david@stfc.ac.uk

[1] W. Grochala and P. P. Edwards, Chem. Rev. **104**, 1283 (2004).
[2] V. Ozolins, E. H. Majzoub, and C. Wolverton, J. Am. Chem. Soc. **131**, 230 (2009).
[3] J.-H. Kim, S.-A. Jin, J.-H. Shim, and Y. W. Cho, J. Alloys Compd. **461**, L20 (2008).
[4] K. Miwa, M. Aoki, T. Noritake, N. Ohba, Y. Nakamori, S. I. Towata, A. Züttel, and S. I. Orimo, Phys. Rev. B **74**, 155122 (2006).
[5] Y. Filinchuk, E. Rönnebro, and D. Chandra, Acta Mater. **57**, 732 (2009).
[6] F. Buchter, Z. Lodziana, A. Remhof, O. Friedrichs, A. Borgschulte, P. Mauron, A. Züttel, D. Sheptyakov, G. Barkhordarian, R. Bormann, K. Chłopek, M. Fichtner, M. Sörby, M. Riktor, B. Hauback, and S. I. Orimo, J. Phys. Chem. B **112**, 8042 (2008).
[7] W. I. F. David, P. C. Aeberhard, and K. Refson (unpublished).
[8] F. Buchter, Z. Lodziana, A. Remhof, O. Friedrichs, A. Borgschulte, P. Mauron, A. Züttel, D. Sheptyakov, L. Palatinus, K. Chlopek, M. Fichtner, G. Barkhordarian, R. Bormann, and B. C. Hauback, J. Phys. Chem. C **113**, 17223 (2009).
[9] M. D. Riktor, M. H. Sørby, K. Chłopek, M. Fichtner, F. Buchter, A. Züttel, and B. C. Hauback, J. Mater. Chem. **17**, 4939 (2007).
[10] Y. Nakamori, K. Miwa, A. Ninomiya, H. Li, N. Ohba, S. I. Towata, A. Züttel, and S. I. Orimo, Phys. Rev. B **74**, 045126 (2006).
[11] Z. Lodziana and M. J. van Setten, Phys. Rev. B **81**, 024117 (2010).
[12] P. Vajeeston, P. Ravindran, and G. H. Fjellvå, J. Alloys Compd. **446**, 44 (2007).
[13] E. H. Majzoub and E. Rönnebro, J. Phys. Chem. C **113**, 3352 (2009).
[14] L. George, V. Drozd, S. K. Saxena, E. G. Bardaji, and M. Fichtner, J. Phys. Chem. C **113**, 15087 (2009).
[15] A. Liu, S. Xie, S. Dabiran-Zohoory, and Y. Song, J. Phys. Chem. C **114**, 11635 (2010).
[16] W. Kohn and L. J. Sham, Phys. Rev. **140**, A1133 (1965).
[17] S. J. Clark, M. D. Segall, C. J. Pickard, P. J. Hasnip, M. J. Probert, K. Refson, and M. C. Payne, Z. Kristallogr. **220**, 567 (2005).
[18] J. P. Perdew, K. Burke, and M. Ernzerhof, Phys. Rev. Lett. **77**, 3865 (1996).
[19] H. J. Monkhorst and J. D. Pack, Phys. Rev. B **13**, 5188 (1976).
[20] D. Vanderbilt, Phys. Rev. B **41**, 7892 (1990).
[21] See supplemental material at [http://link.aps.org/supplemental/10.1103/PhysRevB.83.174102] for details on the vibrational frequency calculations.
[22] K. Refson, P. R. Tulip, and S. J. Clark, Phys. Rev. B **73**, 155114 (2006).

[23] A. M. Rappe, K. M. Rabe, E. Kaxiras, and J. D. Joannopoulos, Phys. Rev. B **41**, 1227 (1990).
[24] V. Swamy, L. S. Dubrovinsky, N. A. Dubrovinskaia, F. Langenhorst, A. S. Simionovici, M. Drakopoulos, V. Dmitriev, and H.-P. Weber, Solid State Commun. **134**, 541 (2005).
[25] P. Y. Simons and F. Dachille, Acta Crystallogr. **23**, 334 (1967).
[26] L. S. Dubrovinsky, N. A. Dubrovinskaia, V. Swamy, J. Muscat, N. M. Harrison, R. Ahuja, B. Holm, and B. Johansson, Nature (London) **410**, 653 (2001).
[27] F. D. Murnaghan, Proc. Natl. Acad. Sci. USA. **30**, 244 (1944).
[28] F. Birch, Phys. Rev. **71**, 809 (1947).
[29] M. Fichtner, K. Chłopek, M. Longhini, and H. Hagemann, J. Phys. Chem. C **112**, 11575 (2008).